Environmental Science and Pollution Research (2020) 27:15068–15082
https://doi.org/10.1007/s11356-020-07835-z

RESEARCH ARTICLE

Co-transport behavior of ammonium and colloids in saturated porous media under different hydrochemical conditions

Jingqiao Li[1,2] · Wenjing Zhang[1,2] · Yunqi Qin[1,2] · Xiaofei Li[1,2] · Shengyu Wu[1,2] · Juanfen Chai[1,2] · Shanghai Du[1,2]

Received: 7 August 2019 / Accepted: 23 January 2020 / Published online: 17 February 2020
© Springer-Verlag GmbH Germany, part of Springer Nature 2020

Abstract

To investigate co-transport behavior of ammonium and colloids in saturated porous media under different hydrochemical conditions, NH_4^+ was selected as the target contaminant, and silicon and humic acid (HA) were selected as typical organic and inorganic colloids in groundwater. Column experiments were then conducted to investigate the transport of NH_4^+ colloids under various hydrochemical conditions. The results showed that because of the different properties of colloidal silicon and HA after combining with NH_4^+, the co-transport mechanism became significantly different. During transport by the NH_4^+–colloid system, colloidal silicon occupied the adsorption sites on the medium surface to promote the transport of NH_4^+, while humic acid (HA) increased the number of adsorption sites of the medium to hinder the transport of NH_4^+. The co-transport of NH_4^+ and colloids is closely related to hydrochemical conditions. In the presence of HA, competitive adsorption and morphological changes of HA caused NH_4^+ to be more likely to be transported at a higher ionic strength (IS = 0.05 m, $CaCl_2$) and alkalinity (pH = 9.3). In the presence of colloidal silicon, blocking action caused the facilitated transport to be dependent on higher ionic strength and acidity (pH = 4.5), causing the recovery of NH_4^+ to improve by 7.99%, 222.25% (stage 1), and 8.63%, respectively. Moreover, transport increases with the colloidal silicon concentrations of 20 mg/L then declines at 40 mg/L, demonstrating that increased concentrations will lead to blocking and particle aggregation, resulting in delayed release in the leaching stage.

Keywords NH_4^+ · Colloid · Hydrochemical conditions · Co-transport

Introduction

Nitrogen in the groundwater occurs in four forms, ammonium (NH_4^+), nitrite (NO_2^-), nitrate (NO_3^-), and organic nitrogen (Mekala and Nambi 2016; Nakasone et al. 2004). The presence of nitrogen is mainly controlled by pH, dissolved oxygen (DO), temperature, and microbial activities (Berlin et al. 2015; Lee et al. 2006). Major transformational processes in different forms in soil and groundwater can be roughly divided into physical, chemical, and biological functions (Behnke 1975) involving nitrification, denitrification (Mekala and Nambi 2016), leaching, biological blockage, and plant absorption (Wang and Alva 2000). Among them, NH_4^+ is the main form in saturated aquifers, originating from landfill and industrial sites leachate, wastewater irrigation, and excessive application of fertilizer (Jellali et al. 2010; Zhai et al. 2017). As the NH_4^+ concentration increases, the ability of aquatic organisms to bind oxygen will be reduced, or even die. Studies have shown that NH_4^+ can be retained in soil or media by cation exchange and adsorption (Jellali et al. 2010; Sprynskyy et al. 2005), and NH_4^+ transport was shown to significantly increase with

Highlights 1. Colloidal silicon facilitated NH_4^+ transport and HA inhibited NH_4^+ transport.
2. The co-transport behavior between NH_4^+ and colloid is subject to different hydrochemical conditions.
3. Main principles include different bonding forms, colloid forms, and charges.

Responsible editor: Philippe Garrigues

Electronic supplementary material The online version of this article (https://doi.org/10.1007/s11356-020-07835-z) contains supplementary material, which is available to authorized users.

✉ Wenjing Zhang
zhangwenjing80@hotmail.com

[1] Key Laboratory of Groundwater Resources and Environment, Ministry of Education, Jilin University, Changchun 130021, China

[2] College of Environment and Resources, Jilin University, Changchun 130021, China

increasing flow rate and concentration (Barnes and Zimniak 1981). In addition, nitrification and denitrification have been confirmed to influence NH_4^+ transport because of biological transformation and pore blocking (Mekala and Nambi 2017). Because NH_4^+ may cause groundwater contamination and serious health issues, additional studies of this compound are of fundamental importance to a variety of applied fields.

Early studies assumed that the transport of contaminants in groundwater involved a mobile liquid phase and an immobile solid phase (Puls and Powell 1992). However, colloids (Buffle and Leppard 1995), as the mobile solid phase, have large specific surface areas and high numbers of reactive functional groups (Kretzschmar et al. 1999) and have been found to be stable in groundwater and capable of being transported over long distances via flow (Xu et al. 2018). Therefore, the presence of mobile colloids will universally act as carriers for the adsorption and transport of contaminants in groundwater (Wang et al. 2016). It is important to note that when colloids are relatively immobile, such as clay colloids, they are more likely to absorb contaminants and thus inhibit transport (Won and Burns 2018; Yin et al. 2018).

The abundance and behavior of colloids in groundwater largely depends on their physicochemical properties, including hydrogeochemical and hydrodynamic conditions (Kretzschmar et al. 1999; Zhai et al. 2019) such as ionic strength (Um and Papelis 2002), pH (Yee et al. 2000), other ions, flow rate, and temperature (Kanti Sen and Khilar 2006). These factors may result in release of colloids by the repulsion force of the double electric layer, variation of shear force, and dissolution of the mineral phase. Colloid transport is known to be affected by diffusion, interception, ripening, and gravity deposition, and its form also affects its adsorption and migration (Zhou et al. 2016). Knappenberger et al. (2015) found there was a difference in retention between spherical and angular colloids in quartz sand columns. In addition, the particle size and zeta potential of colloids have been shown to be important indicators of the stability of colloids (Chrysikopoulos and Katzourakis 2015). Wang et al. (2012) also showed that colloidal silicon with small particle size tended to aggregate and be retained more easily.

Transport of contaminants is often said to be facilitated when associated with colloids through ion exchange, complexation, and hydrophobic partitioning (Kanti Sen and Khilar 2006). A large number of experimental studies have indicated that colloids have a certain effect on the transport of heavy metals and their cations such as Cd (Li and Zhou 2010), Fe (Li et al. 2019), Sr (Bekhit et al. 2006), and Pb^{2+} (Daniel 2005; Yin et al. 2010). Groundwater environments are often subjected to strong variations in hydrodynamic and hydrochemical conditions, and transport of colloids and contaminants is also influenced by these changes. For instance, our previous study showed that Fe and colloids have different co-transport behaviors in the presence of other cations (Li et al. 2019). Moreover, (HA) is generally considered to affect contaminant transport by increasing the effective adsorption point on the surface of solid phases (ripening) (Koju et al. 2019; Yates and Von Wandruszka 1999), but the transport mechanism varies with pH value, which probably occurs because of the morphology of HA (Wang et al. 2013). Humic acid presented the shape of aggregation and the particle size is larger under acid condition (de Melo et al. 2016), which can generate blocking and inhibit migration. However, under alkaline conditions, it is not easy to deposit because deprotonated functional groups cause HA to be linear and have an unfolded chain structure (Colombo et al. 2015; Ma et al. 2018); hence, it is more likely to combine with contaminants and promote transport.

In view of the limited research conducted to date and the potential adverse effects of excessive ammonium in groundwater, investigations of the transport and retention of NH_4^+ with colloids in an underground environment are necessary. Because differences in interionic valence states have a significant impact on co-transport, this study added low ions part to explore their differences relative to high ions. The object of our study was to investigate the co-transport of colloids and NH_4^+ under different hydrochemical conditions using a column transport experiment. HA and colloidal silicon were chosen as typical organic and inorganic colloids, respectively. Zeta potential and particle size distribution were also used to characterize the interactions between colloids and NH_4^+. Experiments were conducted using different media, colloids and concentrations, pH, ionic strength (IS), and cationic valence states, and the results of NH_4^+ transport in the presence of colloids were described by breakthrough curves (BTCs). The results presented herein further improve the understanding of co-transport between contaminants and colloids.

Materials and methods

Experimental materials

Porous media

Glass beads, quartz sand (purchased from Aladdin Reagents, Shanghai), and natural sand with an average diameter of 0.45 mm were selected as the column packing material. Three kinds of porous media were selected to eliminate uncertainties in the transport behavior of colloidal HA and SiO_2 through porous media caused by

heterogeneity and differing interface properties in natural soil. Before filling the column, all porous media was sterilized at high temperature to exclude the effects of nitrification and denitrification, then flushed and ultrasonicated until the impurities were eliminated. After impurity removal, three types of sand were soaked in 0.1 M NaOH (aq) and 0.1 M HNO_3 (aq) in sequence for about 3 h, then washed with deionized water until the pH of the effluent was stable. Finally, all sands were dried at 105 °C for 8 h. The properties of the porous media are given in Table 1.

Preparation of colloid suspensions

Colloidal HA (Tianjin Guangfu Fine Chemical Research Institute, Tianjin, China) and silicon dioxide (Aladdin Reagents) were separately represented as the organic and inorganic colloidal suspensions. Because the two types of colloid particles strongly affected the transport of NH_4^+, they were both used in the column transport experiments.

To remove impurities and non-colloidal particles, colloidal HA was first dissolved in 0.1 mol/L NaOH solution to adjust the pH to 7 ± 0.1, then ultrasonically dispersed for 1 h and passed through a 0.45-μm sieve (Colombo et al. 2015). The resulting suspension was then sonicated for 30 min to disaggregate and disperse the particles, after which it was washed with deionized water until the pH stabilized. The prepared suspensions were subsequently stored in the dark at 4 °C until use. The procedure of preparing silicon colloid was in accordance with the colloidal HA. According to the concentration in the aquifer recharge and the chemical composition of HA and colloidal silicon, the concentration of colloidal HA suspension and colloidal silicon was diluted to 20 mg/L for transport experiments.

Preparation of other suspensions

Three kinds of suspensions were used in the column experiments, background suspensions, experimental suspensions, and the test solution. Background suspensions were prepared with colloid suspension, cation solution, and deionized water and for the column transport experiments, wherein adding 2.93 g/L NaCl or 1.85 g/L $CaCl_2$ can adjust IS = 0.05 M in suspensions. Experimental suspensions were prepared in accordance with background suspensions with respect to the type and concentration of colloid particles, the IS, and the cation valence. Additionally, 2 mg/L of NH_4^+ solutions was diluted by adding standard solutions to the defined amount of deionized water. Sodium potassium tartrate and Nessler reagent were used as the test solutions. The zeta potential and particle size distribution of all suspensions under various hydrochemical conditions were measured by a Zetasizer Nano (Malvern Instruments, UK).

Experimental method

Glass chromatography columns (10 cm long and 3 cm of inner diameter) were used for the transport experiment. A BT-100 peristaltic pump (Longer Pump, Beijing, China) was used to pump an aqueous particle suspension through the packed column at a constant speed. Before each experiment, the packed column was saturated by successive injection with deionized water from bottom to top for 12 h at a low rate of 0.2 mL/min (in keeping with a Darcy velocity of approximately 0.9 m/day) while preventing air bubbles from entering. Moreover, the pH and conductivity (EC) were monitored in real time using a data collector during the saturation stage, which exceeded 12 h (Zhou and Cheng 2018). During this time, two stages of the experiment were performed. In one, the experimental suspension was injected at a speed of 0.5 mL/min for 300 min (10.7 pore volumes, stage 1) to investigate the co-transport between colloids and NH_4^+, while in the other, the background suspension was injected for 750 min (26.8PV, stage 2) (Yin et al. 2018). A magnetic stirrer was used to minimize precipitation during the injection process. To simulate the groundwater environment, the column and the experimental suspensions were kept in an incubator at 10 °C. Finally, a UV-VIS spectrophotometer was used to estimate the concentration of NH_4^+ and colloids according to pre-established calibration curves. All groups of suspensions under different porous media, colloid concentration, IS, and pH

Table 1 Properties of porous media

Porous media	Average size (mm)	Specific surface area (m^2/g)	Porosity	TOC (mg/g)	Components (%)					
					SiO_2	Na_2O	CaO	MgO	Fe_2O_3	Al_2O_3
Glass bead	0.45	0.07	0.42	0.386	75.29	13.26	7.15	4.30	-	-
Quartz sand	0.45	0.16	0.40	0.409	> 99.7	-	-	-	0.10	0.10
Natural sand	0.45	0.24	0.39	2.533	77.30	-	-	-	13.26	9.44

conditions were introduced into the columns. Effluent samples were collected every 15 min using an automatic fraction collector, and the NH_4^+ concentration in each sample was determined by ultraviolet (UV) spectrophotometry. Finally, the colloidal HA suspension under different pH and media conditions was selected as the representative suspension, and its surface morphology was observed by scanning electron microscopy (SEM).

Results and discussion

Physicochemical properties of NH_4^+–colloid suspensions

When inorganic colloidal silicon and organic HA colloids exist, the physicochemical properties of NH_4^+ change significantly, affecting the transport of NH_4^+ in porous media. Under these conditions, the zeta potential and hydrodynamic size are important indexes for evaluation of colloid stability (Maier and Schure 2018). In this study, the zeta potential and hydrodynamic sizes (in Figs. 1, 2, and 3) of NH_4^+ under different IS, cation valences, and colloidal concentrations were determined by using a Marvin instrument (Malvern, UK).

Size of NH_4^+–colloid

As shown in Fig. 1, the hydrodynamic size of colloidal silicon and HA was about 180.7 nm and 155.4 nm, respectively, and only one peak appeared when NH_4^+ was added. Overall, as the colloid concentration was enhanced, the hydrodynamic size increased by 18.76% and 11.27% in the NH_4^+–colloidal silicon and NH_4^+–colloidal HA

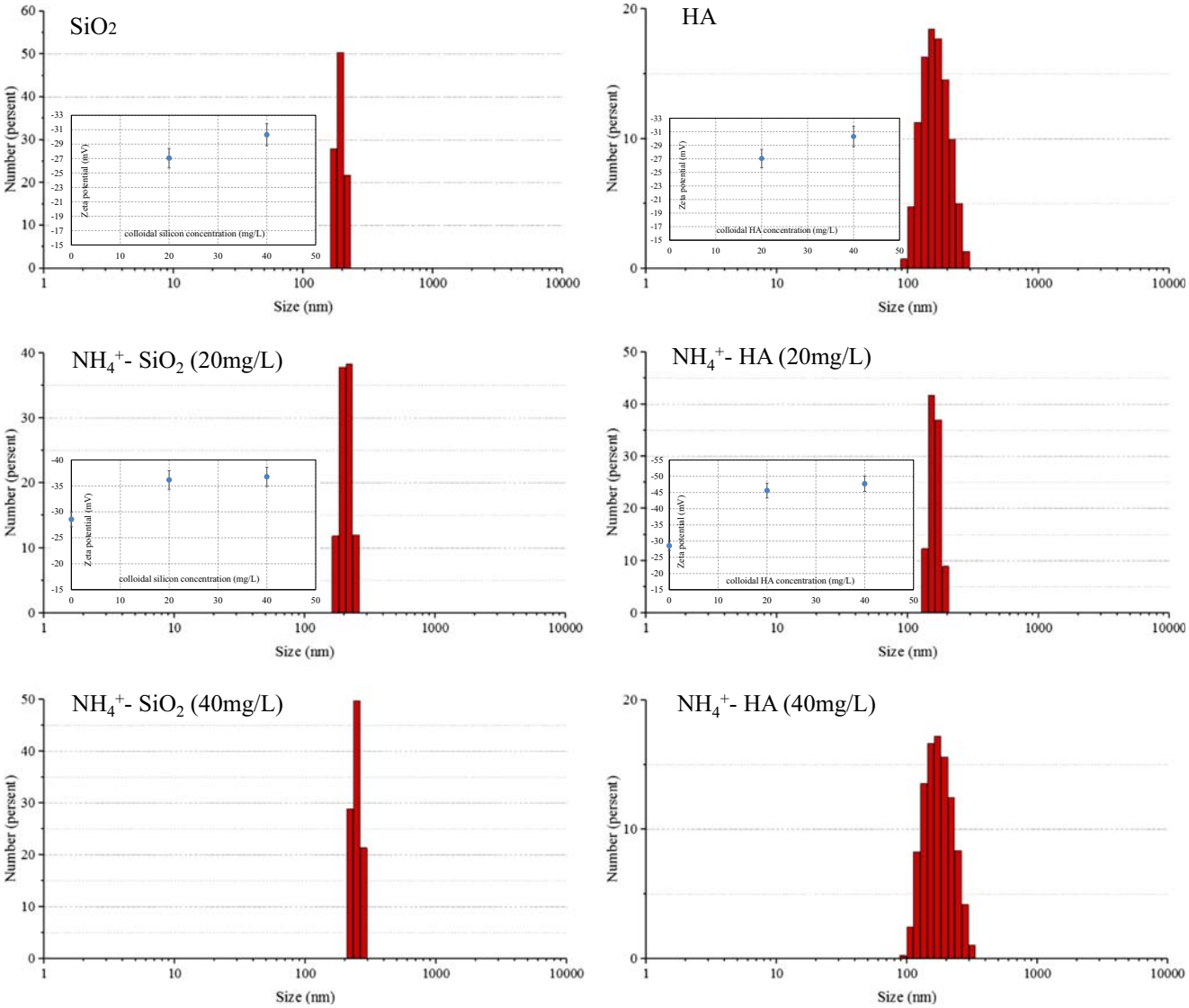

Fig. 1 Hydrodynamic sizes and zeta potentials of single colloid and NH_4^+–colloid systems under different colloid concentration conditions

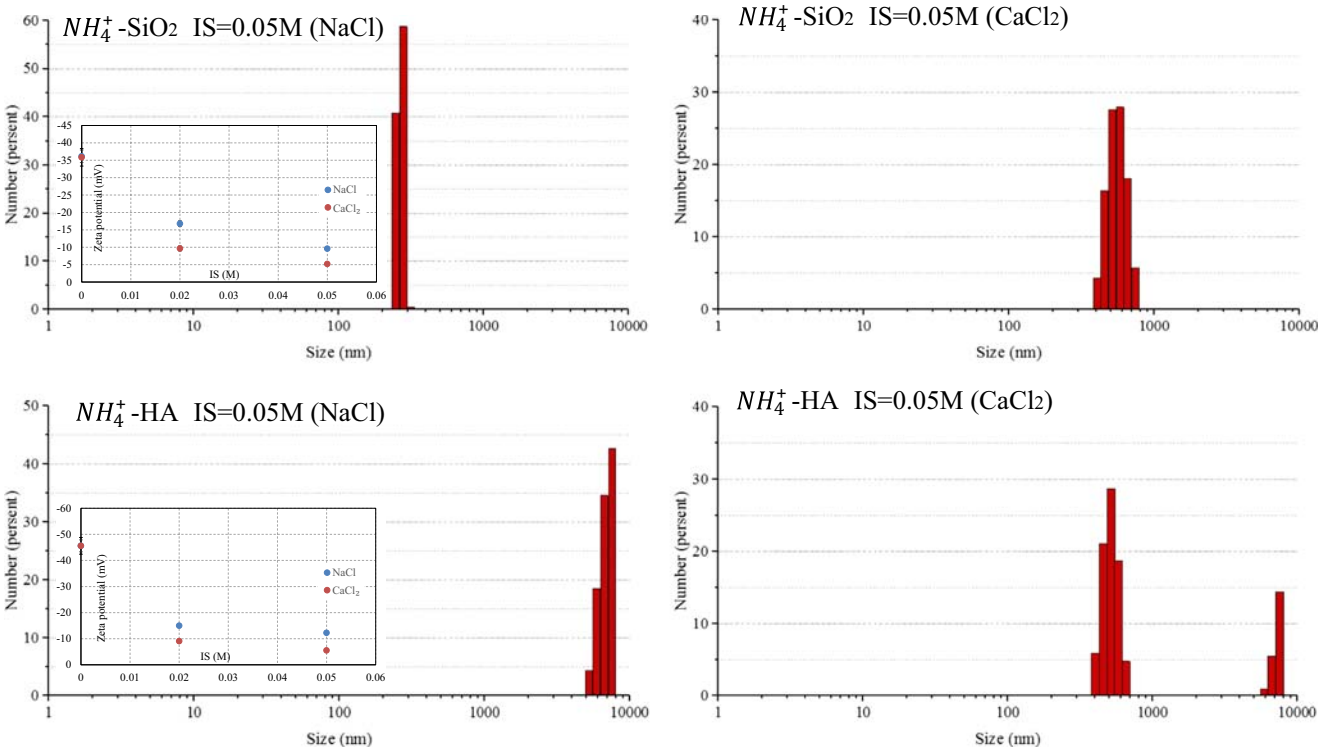

Fig. 2 Hydrodynamic sizes and zeta potentials of single colloid and NH_4^+–colloid systems under different IS conditions

system, respectively. These findings are consistent with those previously reported by our group (Li et al. 2019); however, the mode of combination is different. Specifically, Fe-silicon systems have two different sized peaks, and the second peak belongs to a combination of silicon and Fe. In this study, NH_4^+ appears in a dissolved state and has a low degree of colloid binding, which can better explain why there is only one size peak in the two

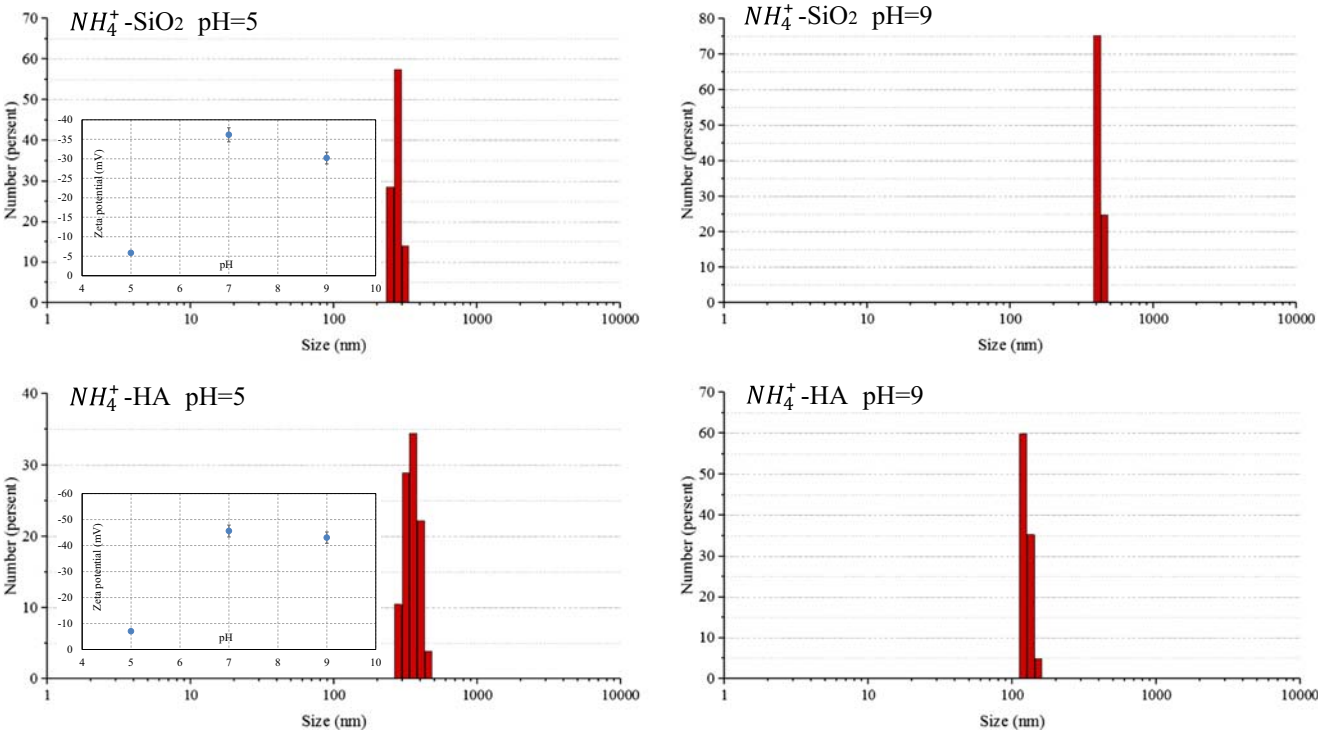

Fig. 3 Hydrodynamic sizes and zeta potentials of single colloid and NH_4^+–colloid systems under different pH conditions

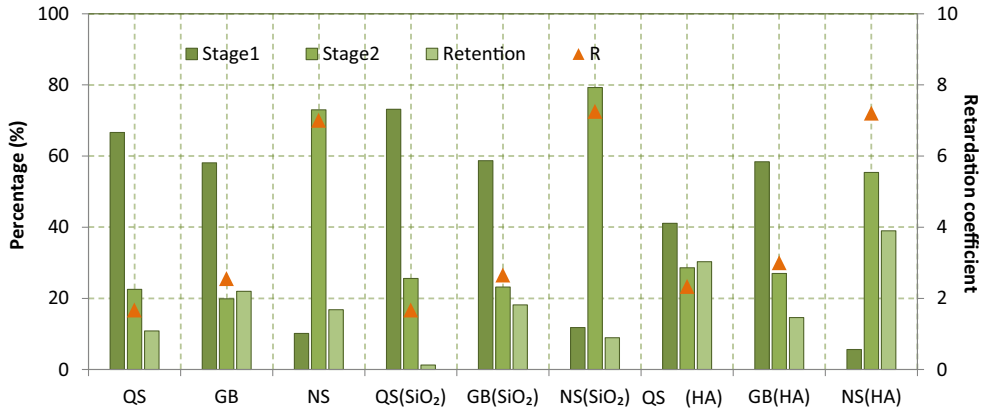

Fig. 4 Column diagram of NH_4^+ transport experiments under different media conditions (1) GB glass beads, QS quartz sand, NS natural sand. (2) Stage 1 Mass recovery in the passing stage. (3) Stage 2: Mass recovery in the leaching stage. (4) Retention (R): Mass retention in the porous media

systems, regardless of the change in colloidal concentration. In addition, the hydrodynamic size increased slightly in the NH_4^+–HA colloid system because under neutral conditions, carboxyl and hydroxyl groups of HA stay between protonated and deprotonated state, which has not much site to combine with other material.

When NaCl or $CaCl_2$ was added into the suspension, the hydrodynamic size tended to increase (Fig. 2). This is probably because the diffusion of the double electric layer of particles is compressed with increasing IS, and the colloid particles are more likely to aggregate under Brownian motion, leading to further increase in hydrodynamic size (Li et al. 2019). Under the same IS condition, the addition of $CaCl_2$ had a more obvious effect on the hydrodynamic size and a second peak appeared in the NH_4^+–HA colloid system. These results indicate that bivalent cations will increase the complexity of the particle bonding state in suspension, leading to aggregation and increased hydrodynamic size, which is consistent with our previous conclusions (Li et al. 2018; Zhou et al. 2017).

Under different pH conditions, the minimum hydrodynamic size in the NH_4^+–colloidal silicon system occurred under neutral conditions, while the maximum size of 390.8 nm was observed under alkaline conditions, which was about twice as large as that under neutral conditions (Fig. 3). This may have been because of the strong influence of pH on the structure of HA. Under alkaline conditions, functional groups of HA such as the phenolic group, hydroxyl group, and carboxyl group were deprotonated, and the repulsive force of groups with negative charge caused HA to show a stretching structure (Ma et al. 2018). Accordingly, hydrodynamic size decreased and aggregation became difficult. However, under acidic conditions, these groups were protonated, which weakened the repulsive force between groups and resulted in a change of HA from a tensile structure to a curly structure (Colombo et al. 2015). This resulted in a larger hydrodynamic size and easier aggregation. Moreover, the presence of functional groups after deprotonation caused HA to more favorably bind to NH_4^+ under alkaline conditions than acidic conditions.

Zeta potentials of NH_4^+–colloid suspensions

According to a previous study, when the absolute value of the zeta potential is greater than 30 mV, the system is considered to be in a stable state (Grolimund et al. 1996). As shown in Fig. 2, the NH_4^+–HA colloid system and NH_4^+–colloidal silicon system were both negatively charged, and the absolute values of the potential of the systems were stable at 35.85 mV and 42.40 mV, respectively. As the colloid concentration increased, the zeta potential of both systems showed an increasing trend. After the addition of HA colloid, the zeta potential of the suspension was greater than that of the system containing added colloidal silicon, indicating that the effects of zeta potential on HA colloids were stronger, and the system

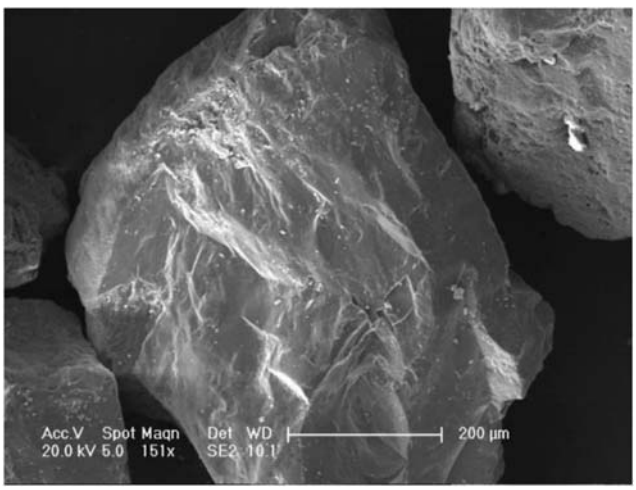

Fig. 5 SEM images of colloidal silicon on natural sand

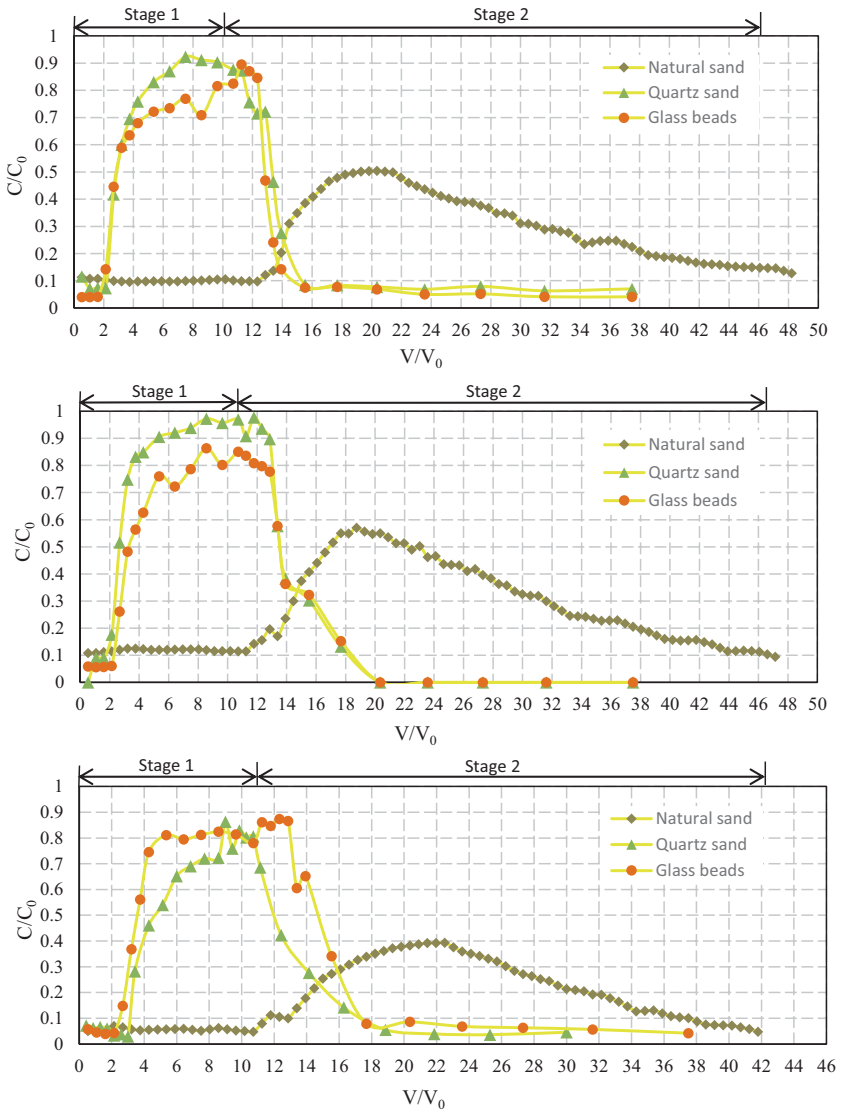

Fig. 6 Breakthrough curves of **a** no colloid, **b** colloidal silicon, **c** and HA under different porous media conditions

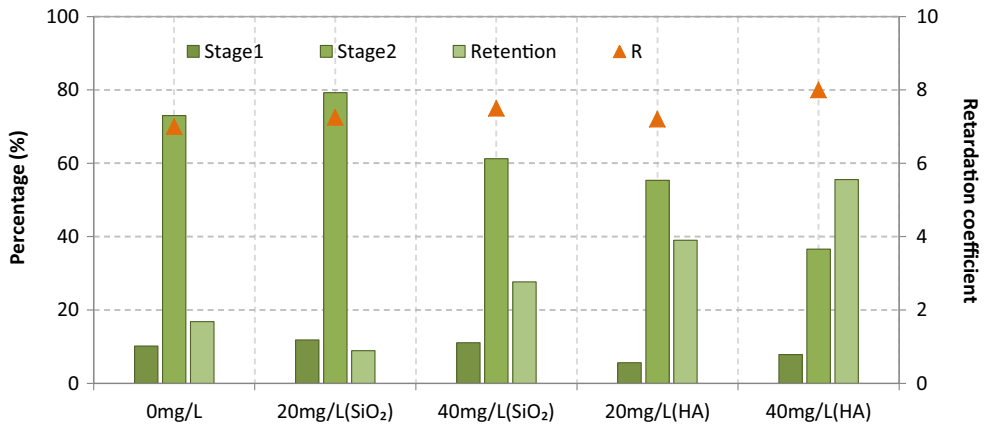

Fig. 7 Column diagram of NH_4^+ transport experiments under different colloid concentrations. Stage 1: Mass recovery in the passing stage. Stage 2: Mass recovery in the leaching stage. Retention (R): Mass retention in the porous media

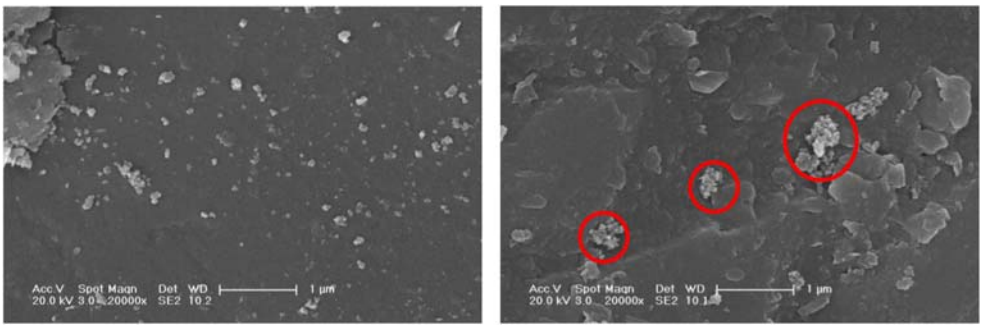

Fig. 8 SEM of colloidal silicon under **a** 20-mg/L and **b** 40-mg/L colloidal silicon concentrations (Aggregates are marked in red)

had high binding rates and remained stable, but there was no phenomenon of charge reversal such as occurs in the Fe-colloidal silicon system (Li et al. 2019).

As shown in Fig. 2, the responses of the NH_4^+–HA colloid system and the NH_4^+–colloidal silicon system to IS changes were roughly the same. Specifically, as IS increased, the zeta potential of both colloidal systems gradually decreased, until finally approaching 5–10 mV, indicating an unstable state. When compared with the conditions of adding two different cation valence states, NaCl always increased the absolute value of the zeta potential more than that of $CaCl_2$; thus, the suspension was more stable after the addition of NaCl. This may have occurred because bivalent cations are more capable of neutralizing negative charges, resulting in a larger positive value of the zeta potential (Liu et al. 2017).

As shown in Fig. 3, the effects of pH on the NH_4^+–HA colloid system and the NH_4^+–silicon system were roughly the same, indicating that the system remained stable under neutral conditions and was unstable under acidic conditions. In the NH_4^+–HA colloid system, the absolute value of the potential was stable under neutral and alkaline conditions, while it was unstable under acidic conditions. However, under neutral and alkaline conditions, the stability of the suspension in the NH_4^+–colloidal silicon system was poorer than that of the NH_4^+–HA colloid system. In general, the stability of the NH_4^+–HA colloid system was better than that of the NH_4^+–colloidal silicon system under all acid-base conditions.

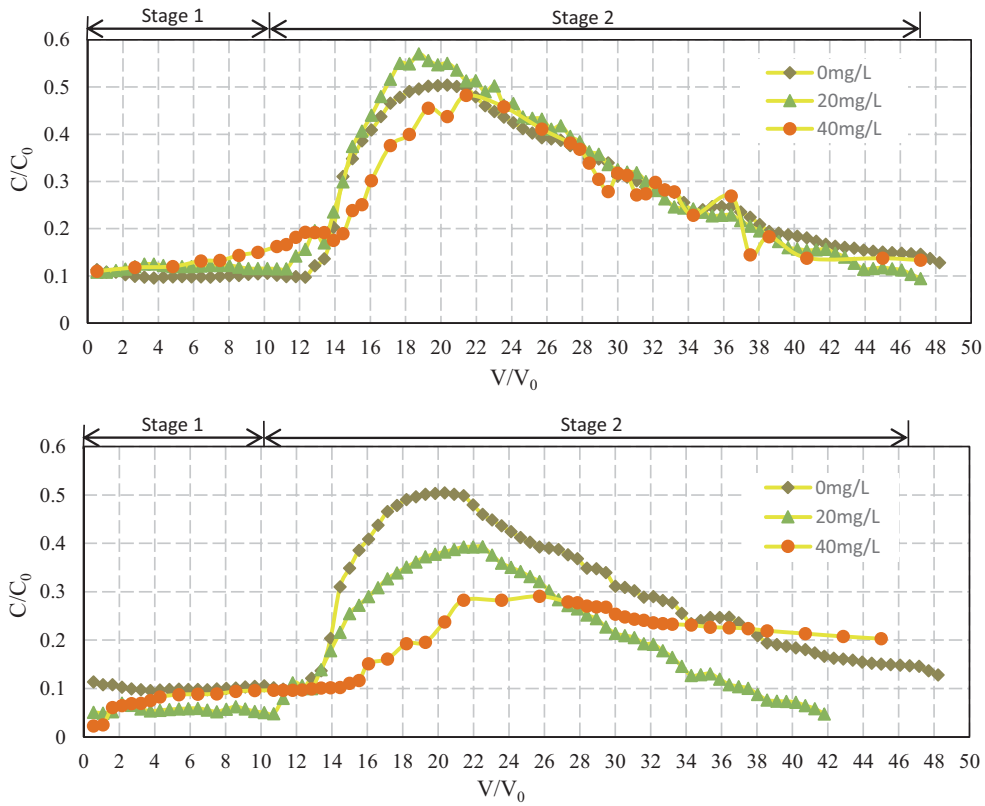

Fig. 9 Breakthrough curves of **a** colloidal silicon and **b** HA under different colloid concentrations

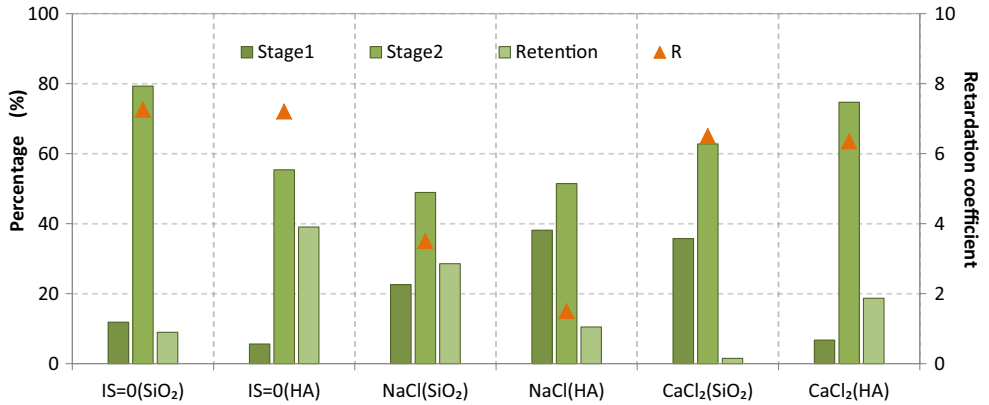

Fig. 10 Column diagram of NH_4^+ transport experiments under different ionic strengths and valence states Stage 1: Mass recovery in the passing stage. Stage 2: Mass recovery in the leaching stage. Retention (R): Mass retention in the porous media

Column transport experiment

NH_4^+ transport in different porous media

The results of NH_4^+ transport through different porous media in the presence and absence of a colloidal system are shown in Figs. 4 and 6.

In the absence of a colloidal system, the recoveries of NH_4^+ in quartz sand, glass beads, and natural sand were 89.15%, 78% and 83.17%, respectively, after the experiment, which did not differ significantly. The BTCs of NH_4^+ in glass beads and quartz sand were similar in shape, but differed greatly from those in natural sand. Overall, NH_4^+ was easiest to transport in quartz sand and most difficult to transport in glass beads.

In natural sand, the peak of C/C_0 was only about half that of the other two media and the recovery of NH_4^+ reached 83.17%. These results were caused by the different properties of natural sand. As shown in Table 1, the specific surface area and TOC of natural sand were both greater than those of the other two kinds of media, indicating that there would be a variety of metal oxide and abundant functional groups on the surface (Ma et al. 2018). These functional groups can provide adsorption sites for NH_4^+, while the presence of metal oxide increases the roughness on the surface of the media, which can enhance the shear resistance during transport. Although NH_4^+ transport in natural sand does not appear the most difficult, as is shown in Fig. 5, it exists obvious hysteresis, and it has been a slow release in the leaching stage, known as reversible adsorption, which can also be seen from the retardation coefficient R. Similarly, because of the smooth surface of glass beads, NH_4^+ migrated most easily. This conclusion is also consistent with the results of our previous research investigating the transport of Fe. Overall, these findings indicate that the physicochemical properties of NH_4^+ are similar to those of metals, which confirms the accuracy.

In the NH_4^+–colloidal silicon system, the shape of the BTCs in the three media was similar to that in the absence of colloids. These findings indicate that colloidal silicon promotes the transport of NH_4^+ in porous media (Vilks and Baik 2001), which is consistent with the results reported by Li. Only 1.27% of the NH_4^+ was retained in quartz sand, indicating that its enhancement of NH_4^+ transport was much greater than that of the other two media. At the end of stage 1, both the glass beads and the quartz sand showed obvious tailing in the BTCs (Bekhit et al. 2006), which was mainly because of the presence of colloids and confirmed that the adsorption of NH_4^+ was reversible (Moradzadeh et al. 2014).

In the NH_4^+–colloidal HA system (Fig. 6), the transport of NH_4^+ in the media was reduced when compared with the absence of colloids. After the experiment, 30.30%, 14.59%, and 39.10% of the NH_4^+ was retained in quartz sand, glass beads, and natural sand, respectively, indicating that NH_4^+ was most likely to be transported in glass beads and most difficult to transport in natural sand. Moreover, the BTCs declined more smoothly and took longer to reach a stable state. These findings indicate that HA colloids generally inhibited the transport of NH_4^+ in porous media. Studies have shown that HA combined with NH_4^+ results in complexation activity (Li et al. 2018). Moreover, natural sand can absorb more HA, resulting in more NH_4^+ adsorption. The mechanism changed from blocking to ripening. As the adsorption sites on natural sand increased, the adsorbed HA concentration increased, hindering the transport of NH_4^+ (Li et al. 2018).

NH_4^+ transport under different colloid concentrations

The NH_4^+ transport is in the presence of 0 mg/L, 20 mg/L, and 40 mg/L colloid and is shown in Figs. 7 and 9.

In the NH_4^+–colloidal silicon system, the peaks of C/C_0 were 0.51, 0.56, and 0.49 at colloid concentrations of 0 mg/L, 20 mg/L, and 40 mg/L, respectively. At a colloidal silicon concentration of 20 mL/L, the final NH_4^+ in the porous media was only 8.92%, which indicated that the existence of colloidal silicon with an appropriate concentration promoted the transport of NH_4^+ in the porous media, but that this facilitation

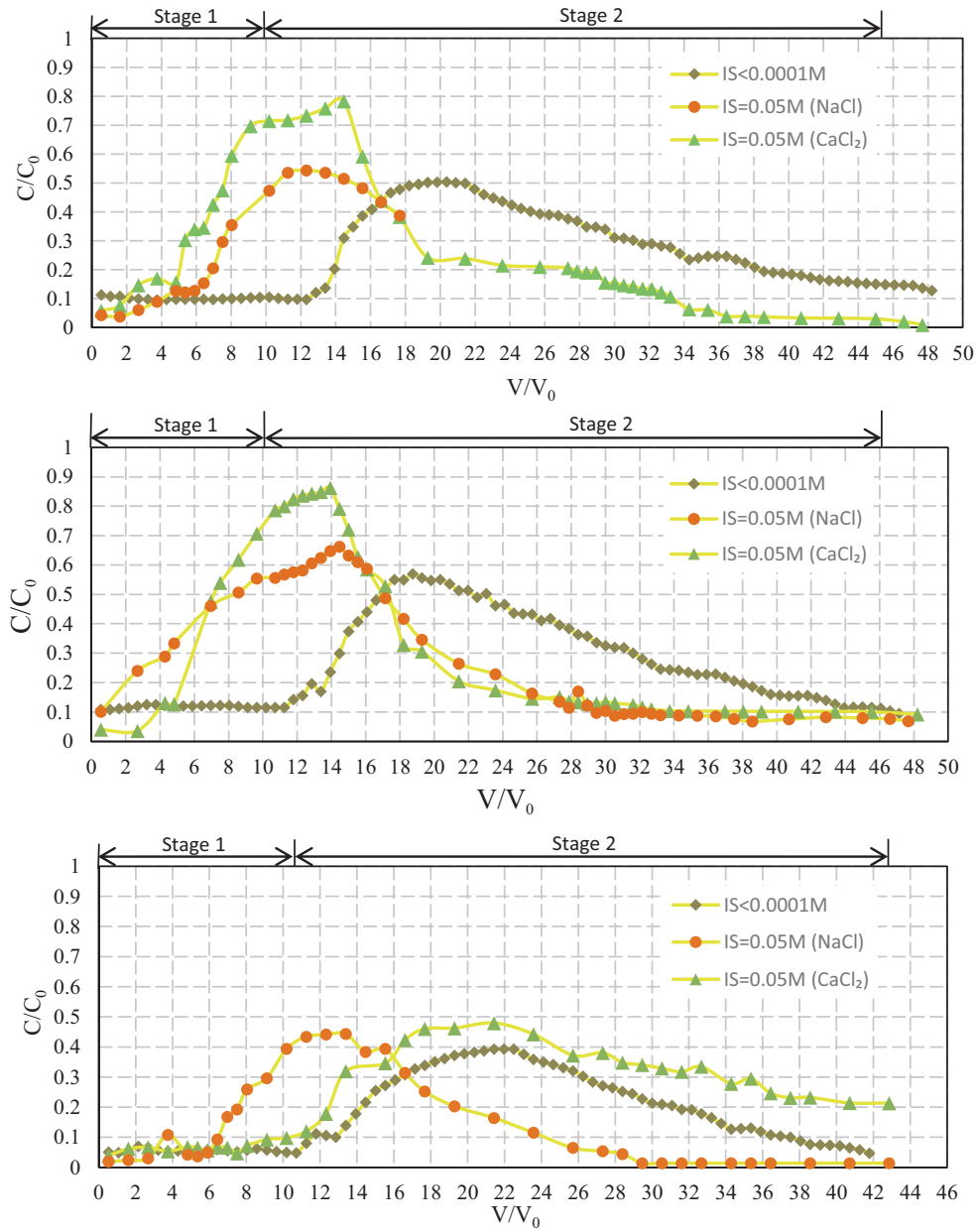

Fig. 11 Breakthrough curves of **a** no colloid, **b** colloidal silicon, and **c** HA under different IS and ionic valence conditions

was limited. Moreover, the concentration of NH_4^+ remained basically stable during the period of 2–11 pv when there were no colloids or low colloid concentrations. This was because the adsorption of NH_4^+ onto porous media under low colloid concentrations manifested as blocking (Wang et al. 2012). The decrease in adsorption sites led to a gradual decrease in adsorption amounts and a slow increase in transport. After adding a colloidal silicon concentration of 40 mL/L, the peak of C/C_0 showed hysteresis and decreased, which was probably because the particles aggregate caused by the increase of colloidal concentration and hydrodynamic size (shown in Fig. 8), but there was still only one distribution peak, indicating that the two kinds of particles achieved a good combination in the suspension. Therefore, it is easy to cause the blocking of media during transport and hysteresis in the leaching stage. Previous studies conducted by our research group have shown that high colloidal silicon concentrations still promote the transport of Fe in porous media, which is contrary to these results. This discrepancy was probably because the bonding rate of Fe and silicon is only 13.3%, while NH_4^+ is more likely to bond in a dissolved state, so NH_4^+ was retained in porous media with colloidal silicon.

With the enhancement of HA concentration (Fig. 9), the retention coefficient R changed from 7.00 to 7.20, suggesting that colloidal HA inhibited the transport of NH_4^+ in the porous media. When the colloid concentration increased to 40 mL/L,

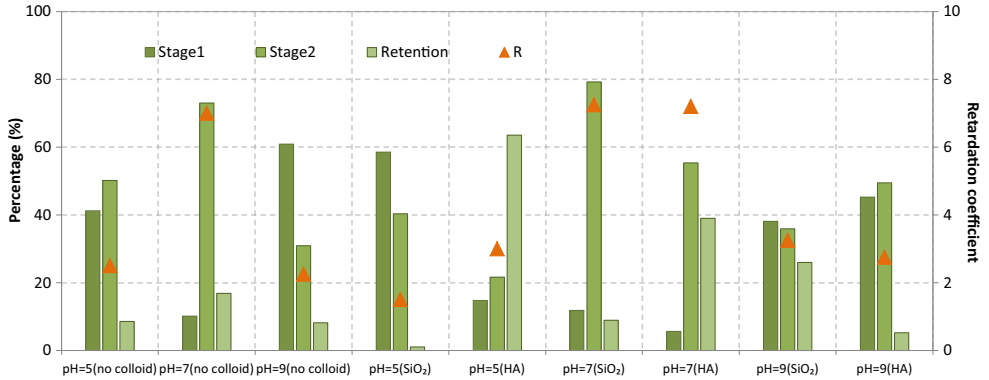

Fig. 12 Column diagram of NH_4^+ transport experiments under different pH. Stage 1: Mass recovery in the passing stage. Stage 2: Mass recovery in the leaching stage. Retention (R): Mass retention in the porous media

the retention effect of NH_4^+ in the transport progress was more obvious, suggesting that within a certain range of colloid concentration, higher levels of colloidal HA led to a more obvious inhibitory effect of NH_4^+ on transport. This was probably because the HA surface had a negative charge. Specifically, negatively charged functional groups can adsorb positively charged NH_4^+, enhancing the ability to bond to particles. Moreover, the more particles that are bound, the stronger its inhibitory effect on transport will be (Xu et al. 2018). Because high HA concentrations can increase the particle size and zeta potential, more NH_4^+ was aggregated and adsorbed in the early stage, and the adsorption was reversible (Yee et al. 2000). Finally, sustained release occurred in the leaching stage.

NH_4^+ transport of different electrolyte valences

The Fe transport through glass beads with different ionic strengths and cationic valences is shown in Figs. 10 and 12.

In the presence of colloidal silicon, the overall trend in BTC was similar to that in the absence of colloids, but the peak was obviously earlier. When NaCl was added, the final retention in natural sand was 10.48%, which was 63.33% less than that in the absence of colloids. These findings indicate that, in the NH_4^+–colloidal silicon system, the addition of NaCl promotes NH_4^+ transport, similar to $CaCl_2$. In addition, as is shown in Fig. 3, $CaCl_2$ in suspension shows a higher hydrodynamic size, which causes blocking in porous media. This is because the diffusion of the double electric layer of particles is compressed, which makes it easier for the colloidal particles to gather together under Brownian motion. $CaCl_2$ has a more obvious promoting effect on NH_4^+ transport because of the increasing ionic strength that occupies the NH_4^+ adsorption sites through the media (Vinogradov et al. 2018). Under this competitive adsorption mechanism, $CaCl_2$ shows stronger competitiveness than NH_4^+ because of its higher valence state, which makes the peak advance more obvious. These findings indicate that increasing ionic strength can promote transport of the NH_4^+–colloidal silicon system.

In the presence of HA colloids, the peak of C/C_0 decreased from 0.54 to 0.44 after the addition of NaCl. At the end of the experiment, NH_4^+ on the media surface accounted for 60.46% of the total, which was more than twice that in the absence of colloids. When $CaCl_2$ was added, the recovery of NH_4^+ finally reached 81.36%. Moreover, compared with IS < 0.0001 M, it can be seen that increasing IS still plays a role in promoting the transport of NH_4^+ in the media but under the condition of HA colloid inhibits the transport of NH_4^+, the promotion effect is not obvious. A high ionic valence state and high ionic strength can promote the transport of contaminants. A

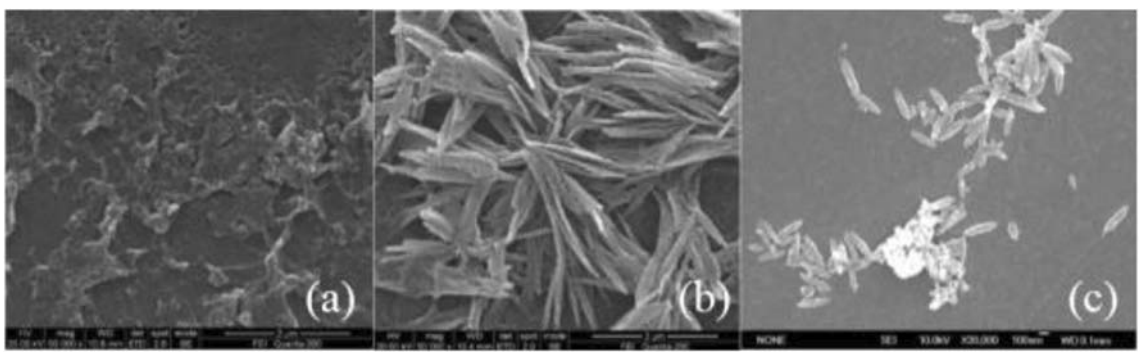

Fig. 13 SEM images of colloidal HA under **a** strong acidity, **b** alkalinity, and **c** weak acidity (Li et al. 2019)

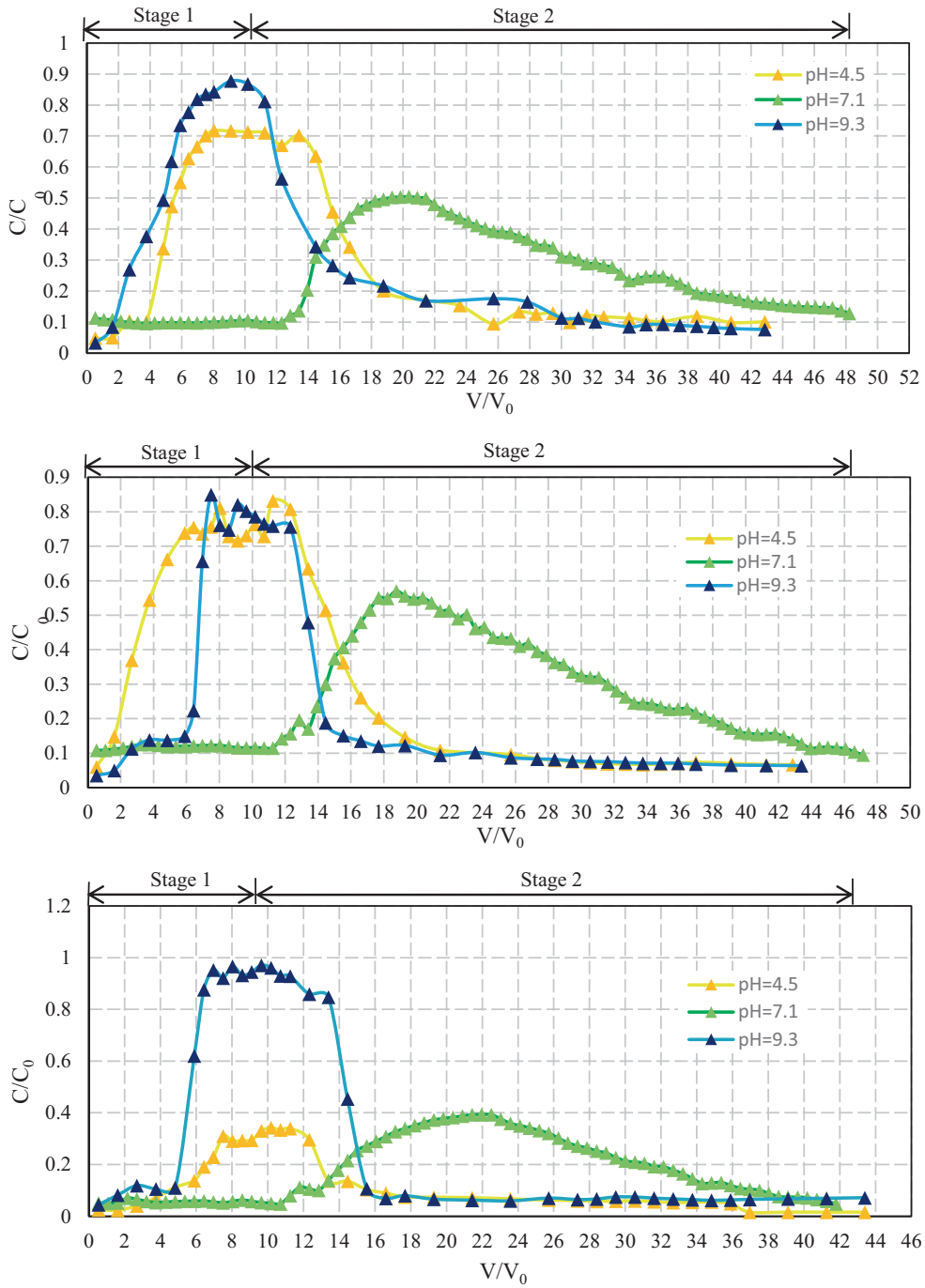

Fig. 14 Breakthrough curves of **a** no colloid, **b** colloidal silicon, and **c** HA under different pH conditions

previous study demonstrated that Ca^{2+} can inhibit the transport of Fe. However, the results now show that Ca^{2+} can promote the transport of NH_4^+. This is because the bivalent cation Ca^{2+} can be considered a low cation with regard to Fe. Competitive adsorption occurs when Fe coexists with Ca^{2+}, and low ions show weaker competition ability. As a result, there is more Fe adsorption on the surface of the media, resulting in inhibitory transport (Yang et al. 2015). Similarly, Ca^{2+} can be considered the high valence cation compared with NH_4^+, and it showed strong ability to compete, reducing the retention of NH_4^+ and promoting transport (Fig. 11).

NH_4^+ transport at different pH

At pH 4.5, when there were no colloids, the peak of C/C_0 was 0.72 at about 10.5 pv, and the recovery of NH_4^+ reached 91.46% in natural sand. In the presence of colloidal silicon, the final total recovery of NH_4^+ increased by 8.18%, which

further confirms that colloidal silicon facilitates transport (Figs. 12 and 13). In addition, the retention coefficient *R* decreased from 7.25 to 1.5, demonstrating that acidic condition (pH = 4.5) can greatly enhance the role of colloidal silicon in promoting the transport of NH_4^+ in the porous media. Under alkaline conditions (pH = 9.3), the hydrogen bonds in the Si-OH group are highly active, which can provide more binding sites for NH_4^+, leading to a hindered effect. Additionally, the zeta potential became lower in the NH_4^+–colloidal silicon system, resulting in reduced stability and increases in hydrodynamic sizes from 196.4 to 390.8 nm. Taken together, these conditions facilitate aggregation on the surface of media, and finally hinder the transport of NH_4^+.

In the presence of HA colloid, the high concentration plain of the BTC decreased significantly, indicating that NH_4^+ transport decreased. NH_4^+ on the media accounted for 63.54% of the total, or nearly eight times that in the absence of colloids. These results indicate that, at pH 4.5, colloidal silicon still promoted the transport of NH_4^+, while HA colloids had the opposite effect. Ripening also occurred under high concentrations. These conclusions are contrary to the finding that HA inhibits NH_4^+ transport under other conditions. This may be because of the deprotonation of hydroxyl and carboxyl functional groups in HA under alkaline conditions, which results in an increase in the repulsive force between these functional groups and leads to production of a long chain–like shape (Knappenberger et al. 2015; Li et al. 2018).

Moreover, according to the new structure, the particle size of HA decreased. More HA colloids combined with NH_4^+ because of the increased binding sites provided by deprotonated functional groups, and HA colloids were relatively easier to transport because of their small particle size and long chain shape (Fig. 14), which is in accordance with the finding that HA colloids promote NH_4^+ transport under alkaline conditions (Ma et al. 2018). When NH_4^+ is transported under acidic and alkaline conditions, the peak of BTCs advanced significantly when compared with neutral conditions. This was mainly because of the introduction of other new ions when adjusting the pH, so NH_4^+ in media exists competitive adsorption.

Conclusions

In this study, the effects of different hydrochemical conditions including media type, colloidal type and concentration, pH, ionic strength, and cation valence state on the physicochemical properties and transport behavior of NH_4^+–colloids were studied. The hydrodynamic size of two colloidal systems increased with increasing colloidal concentration. Additionally, the zeta potential of both systems increased with increasing colloidal concentration, decreasing IS and the neutral condition. The stability of NH_4^+–colloidal HA system was better than that of the NH_4^+–colloidal silicon system.

High concentrations of silicon (40 mg/L) inhibited the migration of NH_4^+ in natural sand, while low concentrations (20 mg/L) promoted its migration. This was mainly because the increase in colloidal concentration caused the aggregation of particles in the suspension, which led to easy blocking and delayed release. Accordingly, higher concentrations of HA colloids led to more obvious inhibitory effects on NH_4^+. The increase of IS promoted the transport of NH_4^+ in natural sand, and the effects of bivalent cations were more remarkable than those of univalent cations because of competitive adsorption. Notably, in the NH_4^+–colloidal HA system, increasing IS still played a role in promoting the migration of NH_4^+, but under the precondition of the inhibitory effect of HA, the promotion effect is not obvious. In addition, acidic conditions promoted the migration of the NH_4^+–colloidal silicon system, while they inhibited the migration of the NH_4^+–colloidal HA system. Under alkaline conditions, the results were reversed. Longitudinal comparison of NH_4^+ migration at pH 4.5, 7.1 and 9.3 revealed that the peaks of BTCs under acidic and alkaline conditions were significantly earlier, mainly because of the introduction of other new ions and the low electronegativity of the NH_4^+–colloidal silicon system and NH_4^+–colloidal HA system.

It should be noted that porous media used in this study were sterilized with high temperature so that nitrification and denitrification could be taken into account in subsequent studies. In addition, only a single hydrochemical condition was used as the control during the experiment. Subsequent studies should include more variables to investigate the co-transport behavior of the NH_4^+–colloidal system.

Acknowledgments The authors appreciate the editors and reviewers for providing valuable advice that greatly improved our paper.

Funding information This work was supported by the National Natural Science Foundation of China (41877175) and the 111 Project [B16020].

References

Barnes EM Jr, Zimniak P (1981) Transport of ammonium and methylammonium ions by Azotobacter vinelandii. J Bacteriol 146(2):512–516

Behnke J (1975) A summary of the biogeochemistry of nitrogen compounds in ground water. J Hydrol 27(1):155–167

Bekhit HM, Hassan AE, Harris-Burr R, Papelis C (2006) Experimental and numerical investigations of effects of silica colloids on transport of strontium in saturated sand columns. Environ Sci Technol 40(17): 5402–5408

Berlin M, Kumar GS, Nambi IM (2015) Numerical modeling of biological clogging on transport of nitrate in an unsaturated porous media. Environ Earth Sci 73(7):3285–3298

Buffle J, Leppard GG (1995) Characterization of aquatic colloids and macromolecules. 1. Structure and behavior of colloidal material. Environ Sci Technol 29(9):2169–2175

Chrysikopoulos CV, Katzourakis VE (2015) Colloid particle size-dependent dispersivity. Water Resour Res 51(6):4668–4683

Colombo C, Palumbo G, Angelico R, Cho HG, Francioso O, Ertani A, Nardi S (2015) Spontaneous aggregation of humic acid observed with AFM at different pH. Chemosphere 138:821–828

Daniel G (2005) Colloid facilitated transport of strongly sorbing contaminants in natural porous media: mathematical modeling and laboratory column experiments. J Environ Sci Technol 17(39)

de Melo BAG, Motta FL, Santana MHA (2016) Humic acids: structural properties and multiple functionalities for novel technological developments. Mater Sci Eng C 62:967–974

Grolimund D, Borkovec M, Barmettler K, Sticher H (1996) Colloid-facilitated transport of strongly sorbing contaminants in natural porous media: a laboratory column study. Environ Sci Technol 30(10): 3118–3123

Jellali S, Diamantopoulos E, Kallali H, Bennaceur S, Anane M, Jedidi N (2010) Dynamic sorption of ammonium by sandy soil in fixed bed columns: evaluation of equilibrium and non-equilibrium transport processes. J Environ Manag 91(4):897–905

Kanti Sen T, Khilar KC (2006) Review on subsurface colloids and colloid-associated contaminant transport in saturated porous media. Adv Colloid Interf Sci 119(2):71–96

Knappenberger T, Aramrak S, Flury M (2015) Transport of barrel and spherical shaped colloids in unsaturated porous media. J Contam Hydrol 180:69–79

Koju NK, Song X, Lin N, Xu KK, Fu H (2019) Enhanced distribution of humic acid-modified nanoscale magnesia for in situ reactive zone removal of cd from simulated groundwater. Environ Pollut 245:9–19

Kretzschmar R, Borkovec M, Grolimund D, Elimelech M (1999) In: Sparks DL (ed) Advances in agronomy. Academic press, pp 121–193

Lee M-S, Lee K-K, Hyun Y, Clement TP, Hamilton D (2006) Nitrogen transformation and transport modeling in groundwater aquifers. Ecol Model 192(1):143–159

Li Z, Zhou L (2010) Cadmium transport mediated by soil colloid and dissolved organic matter: a field study. J Environ Sci 22(1):106–115

Li Y, Koopal LK, Xiong J, Wang M, Yang C, Tan W (2018) Influence of humic acid on transport, deposition and activity of lysozyme in quartz sand. Environ Pollut 242:298–306

Li X, Zhang W, Qin Y, Ma T, Zhou J, Du S (2019) Fe–colloid cotransport through saturated porous media under different hydrochemical and hydrodynamic conditions. Sci Total Environ 647:494–506

Liu D, Zhou JJ, Zhang WJ, Huan Y, Yu XP, Li FL, Chen XQ (2017) Column experiments to investigate transport of colloidal humic acid through porous media during managed aquifer recharge. Hydrogeol J 25(1):79–89

Ma J, Guo H, Lei M, Li Y, Weng L, Chen Y, Ma Y, Deng Y, Feng X, Xiu W (2018) Enhanced transport of ferrihydrite colloid by chain-shaped humic acid colloid in saturated porous media. Sci Total Environ 621:1581–1590

Maier RS, Schure MR (2018) Transport properties and size exclusion effects in wide-pore superficially porous particles. Chem Eng Sci 185:243–255

Mekala C, Nambi IM (2016) Transport of ammonium and nitrate in saturated porous media incorporating physiobiotransformations and bioclogging. Bioremediat J 20(2):117–132

Mekala C, Nambi IM (2017) Understanding the hydrologic control of N cycle: effect of water filled pore space on heterotrophic nitrification, denitrification and dissimilatory nitrate reduction to ammonium mechanisms in unsaturated soils. J Contam Hydrol 202:11–22

Moradzadeh M, Moazed H, Sayyad G, Khaledian M (2014) Transport of nitrate and ammonium ions in a sandy loam soil treated with potassium zeolite – evaluating equilibrium and non-equilibrium equations. Acta Ecol Sin 34(6):342–350

Nakasone H, Abbas MA, Kuroda HJP, Environment W (2004) Nitrogen transport and transformation in packed soil columns from paddy fields. 2(3):115–124

Puls RW, Powell RM (1992) Transport of inorganic colloids through natural aquifer material: implications for contaminant transport. Environ Sci Technol 26(3):614–621

Sprynskyy M, Lebedynets M, Terzyk AP, Kowalczyk P, Namieśnik J, Buszewski B (2005) Ammonium sorption from aqueous solutions by the natural zeolite Transcarpathian clinoptilolite studied under dynamic conditions. J Colloid Interface Sci 284(2):408–415

Um W, Papelis C (2002) Geochemical effects on colloid-facilitated metal transport through zeolitized tuffs from the Nevada Test Site. Environ Geol 43(1–2):209–218

Vilks P, Baik M-H (2001) Laboratory migration experiments with radionuclides and natural colloids in a granite fracture. J Contam Hydrol 47(2):197–210

Vinogradov J, Jackson MD, Chamerois M (2018) Zeta potential in sandpacks: effect of temperature, electrolyte pH, ionic strength and divalent cations. Colloids Surf A Physicochem Eng Asp 553:259–271

Wang FL, Alva AK (2000) Ammonium adsorption and desorption in sandy soils. Soil Sci Soc Am J 64:1669–1674

Wang C, Bobba AD, Attinti R, Shen C, Lazouskaya V, Wang L-P, Jin Y (2012) Retention and transport of silica nanoparticles in saturated porous media: effect of concentration and particle size. Environ Sci Technol 46(13):7151–7158

Wang D, Zhang W, Zhou D (2013) Antagonistic effects of humic acid and iron oxyhydroxide grain-coating on biochar nanoparticle transport in saturated sand. Environ Sci Technol 47(10):5154–5161

Wang Z, Zhang WJ, Li S, Zhou JJ, Liu D (2016) Transport of silica colloid through saturated porous media under different hydrogeochemical and hydrodynamic conditions considering managed aquifer recharge. Water 8(12):14

Won J, Burns SE (2018) Role of immobile kaolinite colloids in the transport of heavy metals. Environ Sci Technol 52(5):2735–2741

Xu N, Cheng X, Zhou K, Xu X, Li Z, Chen J, Wang D, Li D (2018) Facilitated transport of titanium dioxide nanoparticles via hydrochars in the presence of ammonium in saturated sands: effects of pH, ionic strength, and ionic composition. Sci Total Environ 612: 1348–1357

Yang X, Zhang Y, Chen F, Yang Y (2015) Interplay of natural organic matter with flow rate and particle size on colloid transport: experimentation, visualization, and modeling. Environ Sci Technol 49(22):13385–13393

Yates LM, Von Wandruszka R (1999) Decontamination of polluted water by treatment with a crude humic acid blend. Environ Sci Technol 33(12):2076–2080

Yee N, Fein JB, Daughney CJ (2000) Experimental study of the pH, ionic strength, and reversibility behavior of bacteria–mineral adsorption. Geochim Cosmochim Acta 64(4):609–617

Yin X, Gao B, Ma LQ, Saha UK, Sun H, Wang GJJoHM (2010) Colloid-facilitated Pb transport in two shooting-range soils in Florida. 177(1):620–625

Yin X, Jiang Y, Tan Y, Meng X, Sun H, Wang N (2018) Co-transport of graphene oxide and heavy metal ions in surface-modified porous media. Chemosphere 218:1–13

Zhai YZ, Zhao XB, Teng YG, Li X, Zhang JJ, Wu J, Zuo R (2017) Groundwater nitrate pollution and human health risk assessment by using HHRA model in an agricultural area, NE China. Ecotoxicol Environ Saf 137:130–142

Zhai YZ, Zheng FX, Zhao XB, Xia XL, Teng YG (2019) Identification of hydrochemical genesis and screening of typical groundwater pollutants impacting human health: a case study in Northeast China. Environ Pollut 252:1202–1215

Zhou Y, Cheng T (2018) Influence of natural organic matter in porous media on fine particle transport. Sci Total Environ 627:176–188

Zhou J, Zhang W, Liu D, Wang Z, Li S (2016) Influence of humic acid on the transport and deposition of colloidal silica under different Hydrogeochemical conditions. Water 9(1)

Zhou JJ, Liu D, Zhang WJ, Chen XQ, Huan Y, Yu XP (2017) Colloid characterization and in situ release in shallow groundwater under different hydrogeology conditions. Environ Sci Pollut Res 24(16): 14445–14454

Publisher's note Springer Nature remains neutral with regard to jurisdictional claims in published maps and institutional affiliations.